Exploring endocrine GH pattern in mice using rank plot analysis and random blood samples

Jie Xu[1,2], Amaury Jean-Marie Bekaert[1], Joëlle Dupont[3], Sarah Rouve[2,4], Isabella Annesi-Maesano[2,4], C Daniel De Magalhaes Filho[1,2], Laurent Kappeler[1] and **Martin Holzenberger[1]**

[1]INSERM U938, Hôpital Saint-Antoine, Bâtiment Kourilsky, 184 rue du Faubourg Saint-Antoine, F-75012 Paris, France

[2]Université Pierre-et-Marie-Curie, 75005 Paris, France

[3]INRA, 37380 Nouzilly, France

[4]INSERM U707, Hôpital Saint-Antoine, F-75012 Paris, France

(Correspondence should be addressed to M Holzenberger; Email: martin.holzenberger@inserm.fr)

Abstract

GH plays important pleiotropic roles in development, growth, metabolism, and aging of vertebrate species. Mouse mutants with altered GH signaling have been increasingly instrumental in studying somatotropic pathophysiology. However, the pulsatile characteristics of GH secretion are difficult to study in mice because catheterization is cumbersome and long-term serial sampling is limited by small body size and blood volume. We therefore developed an approach routinely applicable to mice, which detects endogenous, physiological GH pattern from randomly obtained spot samples. We determined individual hormone concentration in large groups of mice, ranked the data by magnitude, and statistically analyzed the resulting profiles. This revealed that the nadir-to-peak distribution of plasma GH concentration in mice was similar to other mammals, and that nycthemeral and sex differences existed as well. We found handling stress to be a potent immediate downregulator of circulating GH. We showed that samples need to be taken within seconds to reflect true endogenous levels, unaffected by stress. GH receptor/Janus kinase 2/signal transducer and activator of transcription 5 activation measured in the liver correlated strongly with plasma GH levels, but peak concentrations did not further increase the pathway activation. We applied this rank plot analysis to the GH-deficient and long-lived brain-specific IGF-1 receptor knockout (bIGF1RKO$^{+/-}$) mouse mutant and found a high proportion of low GH concentrations, indicative of extended trough periods and rare peaks. Taken together, we showed that rank plot analysis is a useful method that allows straightforward studies of circadian endogenous GH levels in mice.

Journal of Endocrinology (2011) **208,** 119–129

Introduction

Endocrine pathophysiology and disease have been extensively modeled in spontaneous mutant and genetically engineered mice. Somatotropic hormone functions were among the first to be explored. More recently, a number of mouse mutants affecting the somatotropic axis have been used to investigate the endocrine regulation of mammalian aging and longevity, revealing that diminished GH/insulin-like growth factor 1 (IGF-1) signaling prolongs lifespan (Kenyon 2001, 2005, Bartke 2003, 2008). This has been shown using spontaneous Prop1$^{df/df}$, Pit1$^{dw/dw}$, and GHRHR$^{lit/lit}$ mutants (Godfrey *et al.* 1993, Brown-Borg *et al.* 1996, Flurkey *et al.* 2001), GH receptor (GHR)/binding protein (BP) knockout (Coschigano *et al.* 2000, 2003), IGF-1R$^{+/-}$ and brain-specific IGF-1 receptor knockout (bIGF1RKO$^{+/-}$) mutants (Holzenberger *et al.* 2003, Kappeler *et al.* 2008), and several insulin receptor substrate knockouts (Taguchi *et al.* 2007, Selman *et al.* 2008). To know more about the pleiotropic roles of endocrine GH in the pathobiology of aging, there is a strong interest to investigate GH secretion in these models. Determining the dynamic pattern of GH release in mice is, however, difficult.

Anterior pituitary somatotroph cells release GH into the blood through coordinated exocytosis following a pulsatile pattern (reviewed in Veldhuis *et al.* (2008) and Fig. 1A and B). Classically, the analysis of GH secretion pattern prevailing in a group of individuals requires establishing the pulsatile GH profile for each individual. This in turn requires measuring GH levels in each individual from a series of blood samples taken at short intervals (5–20 min). These samples must be taken over long periods, at least 8–10 h, to include several peaks and nadir levels, or over 24 h to allow identification of nycthemeral pattern. With this approach, the physiology of GH release has been extensively studied in humans and rats (Giustina & Veldhuis 1998). In contrast, elucidating GH pulsatile patterns in mice remains very challenging. First, because the microsurgery for venous catheterization is hazardous in small animals, in particular in growth-deficient mouse mutants, and secondly, because

DOI: 10.1677/JOE-10-0317
0022–0795/11/0208–119

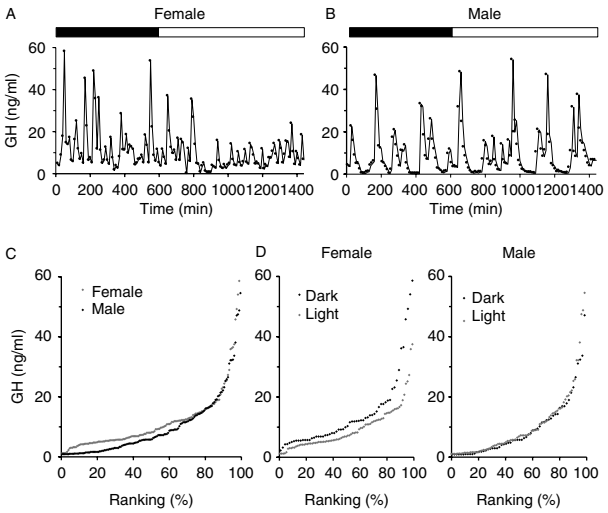

Figure 1 Comparison of time series with rank plot. (A and B) show typical individual 24 h GH profiles of one male and one female rat, taken from Pincus *et al.* (1996). The first 600 min correspond to the dark period, and 600–1440 min to the light period. (C) Ranked distribution of the data in (A and B) confirmed low nadir and intermediate GH levels in the male compared with the female individual ($P<0{\cdot}005$; the Wilcoxon rank test). (D) On average, GH during the dark period was higher than during the light period in the female ($P<0{\cdot}005$; log-rank test), whereas no difference was observed in the male.

the small blood volume of mice strongly limits the number of samples that can be taken from the same individual. While larger animal species allow frequent sampling of plasma over 24 h, only one group reported on a serial sampling for GH determination in mice over 8 h (MacLeod *et al.* 1991, Pampori & Shapiro 1994). On the other hand, much of the recent data on mammalian somatotropic pathophysiology have been generated in mouse models. Thus, a more easily applicable method to investigate GH release in mice would be extremely helpful.

To this end, we developed a strategy to assess GH pulsatility without catheterization and serial sampling. Instead, we determined peripheral GH in blood samples obtained randomly over 24 h from a large cohort of mice. We then arranged the GH values in order of magnitude as a rank plot. These values represent proportionally the various features of a GH pulsatile curve, i.e. nadir, large and small peaks, and intermediate phases, and thus we obtained a useful readout of the underlying pulsatile pattern. Rank plot data were then submitted to statistical analysis. To validate this protocol, we transformed the published data on pulsatile GH in rats (Pincus *et al.* 1996) from serial to rank plot. We also showed that rank plot efficiently reveals the key features of various simulated pulsatile GH profiles. Moreover, when we applied this approach to normal mice, it detected known effects of stress and circadian rhythm on circulating GH. We also used rank plot analysis to investigate the GH pattern in bIGF1RKO$^{+/-}$ mice (Kappeler *et al.* 2008) and found this long-lived mutant had extended trough periods and rarefied peaks.

Materials and Methods

Mice

C57Bl/6 (*B6*) and 129/Sv (*129*) mice were obtained from Charles River Laboratories (CRL, L'Arbresle, France). *Igf1r*$^{flox/+}$ mice (Kappeler *et al.* 2008) were maintained in *129* genetic background for >15 generations. The Nestin-Cre (*NesCre*) transgene was maintained in C57Bl/6 (*B6*) mice for >15 generations. It produces Cre recombinase in neural and glial precursors during early neural development (Tronche *et al.* 1999). We mated *NesCre*$^{+/0}$ males with *Igf1r*$^{flox/flox}$ females to produce an F1 hybrid cohort on a *129/B6* genetic background, composed of heterozygous bIGF1RKO$^{+/-}$ mice and their wild-type littermate controls. Animals lived under specific pathogen free conditions in ventilated cages (Tecniplast, Milan, Italy) at 23 °C, with a 14 h light:10 h darkness cycle. Ventilated cages provide sufficient olfactory and acoustic isolation from the environment, such that the simple presence of humans in the animal room is not stressful for animals. Mice had free access to water and a commercial rodent diet. We separated mice from mothers on day 30 and housed six males or six females per cage, each cage containing three control and three mutant animals. Cages were equipped with a mouse house (Tecniplast) to enhance social interaction and prevent male aggressiveness. We conducted experiments following the institutional guidelines for the care of laboratory animals.

Genotyping

We genotyped mice by multiplex PCR using DNA from skin biopsies. Primers, 5′-CCATGGGTGTTAAATGTAA-TGGC-3′, 5′-ATGAATGCTGGTGAGGGTTGTCTT-3′, and 5′-ATCTTGGAGTGGTGGGTCTGTTTC-3′, were used to amplify DNA from wild-type (256 bp), floxed (312 bp), and Cre-lox recombined (204 bp) *Igf1r* alleles. We detected the transgene *NesCre* using Cre cDNA primers 5′-CCTGGAAAATGCTTCTGTCCG-3′ and 5′-CAGG-GTGTTATAAGCAATCCC-3′ (392 bp), and Gabra1 primers 5′-AACACACACTGGCAGGACTGGCTAGG-3′ and 5′-CAATGGTAGGCTCACTCTGGGAGATGATA-3′ (292 bp) as positive PCR control.

Blood sampling and GH RIA

GH secretion follows both nycthemeral and ultradian patterns. To detect such patterns, we collected blood samples at regular 40 min intervals over 24 h. At the time of sampling, mice were, on average, 16 weeks old, the youngest being 13 and the oldest 19 weeks old. To reduce the number of animals, but also to allow for immediate sample processing and to check for reproducibility, we performed this experiment in three sessions with a 10-day interval between them. During the first session, the mice were sampled at 0800, 1000, 1200 h, etc. the second session at 0840, 1040, 1240 h, etc. and

the third session at 0920, 1120, 1320 h, etc. At each time point, we drew blood from all six males and six females from two randomly chosen cages. Ocular sinus blood (250 μl) was collected from vigil adults using topical anesthesia and EDTA anticoagulant. For each cage, samples were taken from the first three animals immediately after opening the cages to obtain samples reflecting unstressed GH concentrations. No time was lost between moving the cage and drawing blood. The remaining three animals were sampled between 3 and 6 min after opening the cages. Using this strategy, we obtained a total of 432 samples from 144 mice (36 wild-type females, 36 bIGF1RKO$^{+/-}$ females, 36 wild-type males, and 36 bIGF1RKO$^{+/-}$ males), half of which were stressed, while the others were unstressed. Whether an individual was assigned to the stressed or unstressed group was random for each of the sessions. We thereby obtained eight groups, with mice being female or male, wild-type or mutant, and unstressed or stressed. Blood samples were immediately cooled on ice, centrifuged within 15 min, and plasma frozen and stored at −25 °C. We measured GH in 100 μl plasma per mouse using rat-specific RIA (Linco, MP Biomedical, Irvine, CA, USA) that also detects mouse GH (Kappeler *et al*. 2009). All samples were processed in the same assay. The sensitivity of the assay is 0·5 ng/ml. All values below this threshold were set to 0·5 ng/ml.

GHRH stimulation test

Adult males received 50 mg/kg i.p. pentobarbital anesthesia. They were injected 20 min later with mouse recombinant GHRH (0·5 mg/kg i.p., Phoenix Pharmaceuticals, Belmont, CA, USA). Blood was sampled either at the time of injection (T0) or 5 min after injection (T5), by retro-orbital puncture.

ACTH induction

ACTH was measured using Bioplex methodology (Bio-Rad). Blood samples were taken between 1000 and 1200 h to minimize any effects due to circadian rhythm. For basal ACTH, blood was sampled from unstressed mice. For stress-induced ACTH, mice were immobilized for 30 min in ventilated restraint tubes (Kent Scientific Corporation, Torrington, CT, USA) where they could not move but could breathe freely.

Tissue sampling and western blotting

To correlate the circulating GH levels with activation of the GHR/Janus kinase 2 (Jak2)/signal transducer and activator of transcription 5 (Stat5) pathway in the liver, we collected blood for RIA immediately after opening the cage, and took liver tissue samples from the same animals after exactly 2 min. Tissue samples for protein extraction were snap-frozen over liquid nitrogen. This experiment was carried out during daylight period. Western blotting was performed as described earlier (Dupont *et al*. 2000). We used anti-phospho-tyrosine (PY20, Transduction Laboratories, BD Biosciences, Franklin Lakes, NJ, USA), anti-mouse GHR (from G Gudmundur and F Talamantes), and anti-mouse pJak2 Tyr1007/1008 (Cell Signaling Technology, Danvers, MA, USA) antibodies. We carried out immunoprecipitation experiments with anti-rabbit Stat5 antibodies (Cell Signaling; Ozyme, Saint-Quentin-en-Yvelines, France) and immunoblotting with PY20 and then Stat5 antibodies to determine tyrosine phosphorylation of Stat5. We confirmed equal loading for each immunoblot. Bound antibody was revealed using peroxidase-conjugated secondary antibodies and ECL (Amersham Pharmacia Biotech). Signals were quantified using MacBas 2.5 (Fujifilm, Bois d'Arcy, France).

Immunohistochemistry

Pituitaries from 3-month-old bIGF1RKO$^{+/-}$ and control males were fixed in 4% paraformaldehyde, embedded in gelatin (Sigma), and frozen. Cryosections (18 μm) were fixed on Superfrost+ slides, and incubated with rabbit anti-GH antibody (NIDDK, National Hormone and Peptide Program), followed by incubation with Alexa-546-conjugated anti-rabbit antibody (Molecular Probes, Invitrogen, Cergy Pontoise, France). Slides were mounted with DAPI Vectashield medium (Vector Laboratories, Burlingame, CA, USA), and micrographs were acquired under identical conditions for light intensity, charge-coupled-device (CCD) image acquisition, and signal integration with a ×60 oil objective using an Olympus BX612 fluorescence microscope and DP71 CCD camera.

Statistical analysis

To rank the GH values, we assigned to each GH concentration observed in a given population the fraction of the population that has a lower GH level, similar to survival analysis. Log-rank test and the Wilcoxon signed-rank test were used to compare ranked GH distributions between the groups. The log-rank test takes account of the entire curve across all GH concentrations giving the same weight to all observations and was used to evaluate differences due to nycthemeral rhythm, stress, and *Igf-1R* gene mutation. The Wilcoxon signed-rank test was used for evaluating sex differences in GH because it takes into consideration preferentially the left end (nadir) of the distribution; χ^2 was used where indicated. The Mann–Whitney *U* test was used for group comparisons of the GHR/Jak/Stat pathway activation. Data showing normal distribution were analyzed by two-tailed Student's *t*-test and the results were expressed as mean ± S.E.M. To estimate the number of samples needed to detect significant differences in rank plot analysis, we 1) constructed a series of pulsatile profiles and 2) applied an algorithm consisting in a random drawing of a chosen number of samples subsequently submitted to log-rank test. Differences were considered significant for $P<0{\cdot}05$.

Results

Rank plot analysis provides a useful readout of pulsatile GH

Pincus *et al.* (1996) explored pulsatile GH in cannulated rats as time series (Fig. 1A and B), revealing sexual dimorphism in GH secretion. In males, large peaks occur regularly throughout the light and dark periods and are separated by long troughs. In females, large peaks occur preferentially during the dark period, with more irregular patterns of GH secretion: females produce frequent smaller peaks and higher trough values than males. We extracted the GH values from a representative male and female rat published by Pincus *et al.*, and arranged them by order of magnitude, from lowest (nadir) to highest GH value (maximum peak; Fig. 1C). This presentation of the GH data shows the relative prevalence of low, intermediate, and high GH levels in blood, and thereby estimates the overall duration of exposure to the various GH concentrations. This ranked distribution can then be used to compare the effects of mutations or treatments on GH. In this example, the rank plot revealed low nadir levels in males ($P<0{\cdot}02$, the Wilcoxon signed-rank test). This difference depended essentially on the GH values below 15 ng/ml, i.e. nadir and intermediate GH levels. In rank plots, intermediate GH levels represent small peaks and the ascending/descending phases of high peaks. We then compared GH levels from the dark period with those from the light period. Rank plot analysis revealed lower GH levels throughout the light period in the female ($P<0{\cdot}005$, log-rank test), while there was no difference in the male (Fig. 1D). Thus, rank plot of the GH data allowed detection of known sex-related and nycthemeral differences.

We then sought to demonstrate how different GH patterns transform into rank plot. We therefore constructed six pulsatile profiles (Fig. 2A and B), representing the different types of GH secretion patterns as they can be observed due to disease, gene mutation, or aging (Pincus *et al.* 1996, Kappeler *et al.* 2004 and data herein). We then transformed these six time series into rank plots, by taking one data point every 5 min and arranging them by magnitude (Fig. 2C and D). The rank plots of these profiles were distinct from the normal pattern. Changes in the frequency of peaks or in their shape translated directly into overall elevated or suppressed GH levels, including marked changes in the proportion of nadir values. Ranked distributions from profiles with higher or lower peaks showed typical differences in the high end of GH values, not in nadir levels. Considering that a typical pulsatile profile comprises 8–10 peaks per day, about 10% of the random spot samples will fall into a peak area (compare with Fig. 1). To detect at least one peak with 95% confidence interval, the required sample size is 29. To detect the differences among various rank plot profiles with $P<0{\cdot}05$, the necessary sample size depends on the relative difference in prevalence of peak values or differences in peak

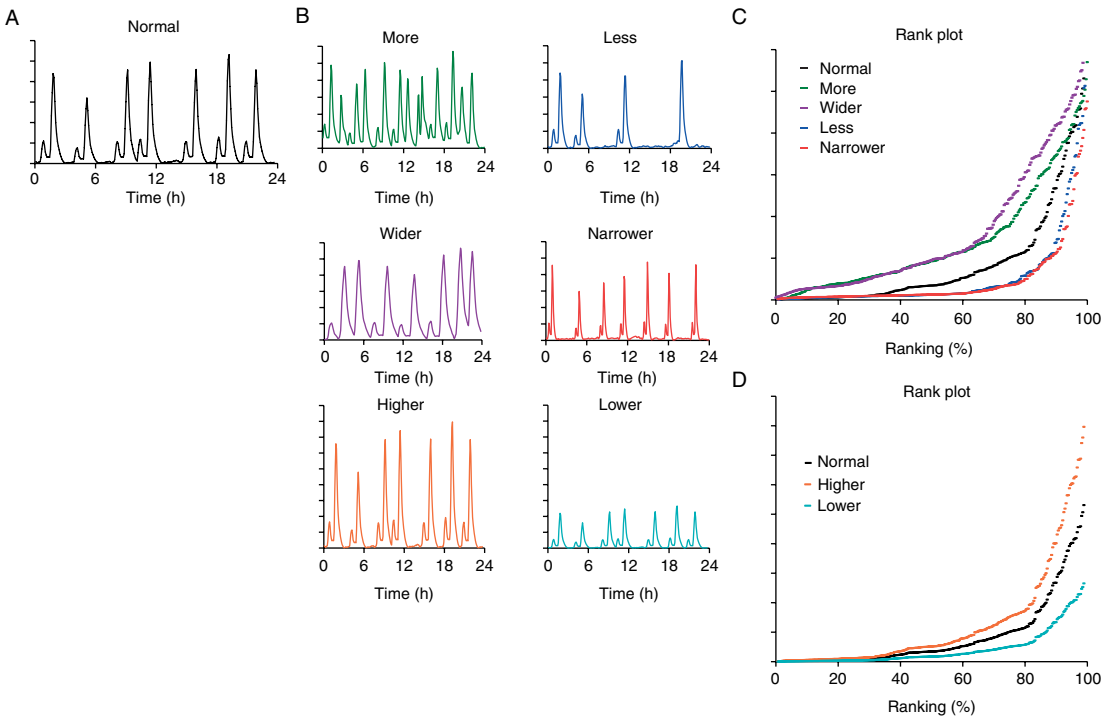

Figure 2 Examples of how simulated GH pulsatile pattern translate into rank plot profiles. (A) Idealized normal GH secretion, with nadir, small peaks, and large peaks. (B) Modified pulsatile patterns with more or less, wider or narrower, higher or lower peaks (color code corresponds to C and D). (C and D) A series of points was collected from each curve in (A and B) and ranked by magnitude. Rank plots highlight key elements of the different serial GH patterns.

height. An estimation of the required sample size for a given series of differences between the groups showed that differences in peak height or frequency in the range of ±30 to ±40% can be revealed with sample sizes between 30 and 100 (Table 1). More subtle differences in the GH distribution require samples sizes above 100. While sample size has a clear impact on statistical power, representative rank plot profiles can be established with as few as 25 samples (Supplementary Figure 1, see section on supplementary data given at the end of this article).

Next, we used rank plot to analyze the GH data obtained in cohorts of wild-type mice. The resulting GH profiles, each representing a large group of animals, were very similar to the profiles from a single male or female rat after serial sample collection (compare Figs 3A and 1C). As in Fig. 1, the distribution in wild-type mice reflected the various phases of GH secretion, i.e. nadirs, intermediate levels, and high peaks. Most values were low, many samples were intermediate, and several high values were also present. GH values from the low range of concentrations were higher in females than in males, suggesting higher nadir levels in females. Moreover, 40% of female GH values were lower than 2·0 ng/ml, compared with 56% in males ($\chi^2=5{\cdot}1$, $P<0{\cdot}01$). As mentioned, GH secretion patterns differ during light and dark periods in many species, including rats (Pincus *et al.* 1996, Giustina & Veldhuis 1998). We therefore compared GH levels from the light period with those from the dark period (Fig. 3B and C). In females, we found that GH was significantly higher during the light period ($P<0{\cdot}05$; log-rank test), while differences in males were not significant. Samples were taken following a randomized 24 h schedule that allowed us to search for the nycthemeral pattern. We found no evidence for synchronization of GH secretion among individuals and no evidence for accumulation of peaks at specific times of the day.

Table 1 Estimation of the number of observations needed for analysis of blood GH using rank plot analysis

Quality of change	**Change** (%)	***n****,[a]
Increased proportion of peaks[b]	+29	93
	+43	21
	+57	<10
	+71	<10
Decreased proportion of peaks[b]	−29	314
	−43	119
	−57	71
	−71	11
Increased height of peaks[b]	+20	248
	+30	116
	+40	54
	+50	40
Decreased height of peaks[b]	−20	146
	−30	53
	−40	38
	−50	32

Number of observations '*n*' required to obtain $P<0{\cdot}05$ using log-rank test.
[a]Individuals can be sampled again after several days interval.
[b]Data for these estimations can be requested from the authors.

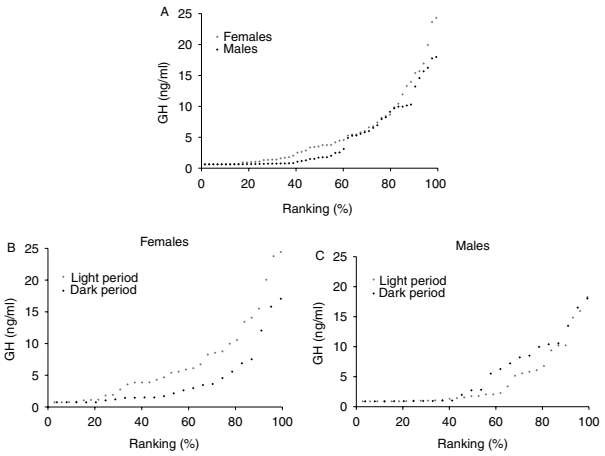

Figure 3 Rank plot of plasma GH in adult wild-type mice (mean age 16 weeks). (A) The overall GH pattern was not significantly different between males and females. Females, $n=56$; males, $n=56$. $P=0{\cdot}23$ (log-rank test). Values correspond to a 24 h sampling interval including light and dark period. (B) GH levels were higher during the light period than during the dark period in females. Dark, $n=24$; light, $n=32$. $P<0{\cdot}05$, log-rank test. (C) In contrast to females, males showed no significant difference in GH levels between the light and dark period. Dark, $n=24$; light, $n=32$; $P=0{\cdot}56$, log-rank test.

Stress rapidly downregulates plasma GH in mice

To demonstrate the effects of physiologically stressful situations on circulating GH, we compared the GH secretion patterns from stressed and unstressed wild-type animals using rank plot analysis. Mice swiftly develop a significant stress reaction when their cage is opened and when they are handled (Balcombe *et al.* 2004). Therefore, in the control group, samples were taken immediately after the cage was opened, so that the GH levels still represented unstressed GH levels; in the stressed group, samples were taken 3 min later, allowing the effects of stress to develop. We found that GH values in the stressed group were predominantly in the nadir range, and that the number of intermediate values was strongly diminished compared with the unstressed (Fig. 4). In females, 75% of the GH values from stressed mice were below 2 ng/ml compared with 40% in the unstressed/control group ($\chi^2=25{\cdot}1$, $P<0{\cdot}001$); in males, 83% from stressed mice compared with 56% from the control group ($\chi^2=17{\cdot}2$, $P<0{\cdot}001$). Peak values were less frequent in stressed animals, but could rise as high as those from unstressed individuals. The overall rank plot pattern was significantly different between stressed and unstressed animals ($P<0{\cdot}001$ in females, $P<0{\cdot}005$ in males, log-rank test; Fig. 4).

Applying rank plot analysis to GH-deficient mice

Next, we applied rank plot analysis to investigate GH activity in a GH-deficient mouse model. We recently reported that bIGF1RKO$^{+/-}$, using Nestin-Cre (Tronche *et al.* 1999)

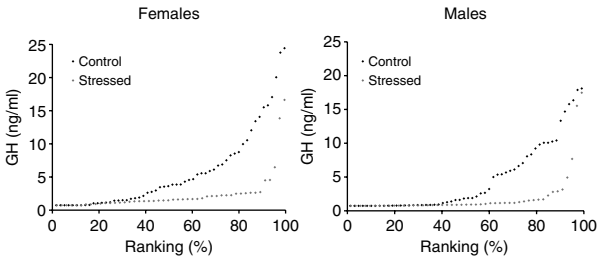

Figure 4 Rank plot showing the effect of stress on GH secretion in adult mice (mean age 16 weeks). To demonstrate the stress response in mice due to cage opening and handling, we took blood immediately after cage opening for half of the mice; these unstressed control values were those presented in Fig. 3. For the other half, blood was taken 3 min after opening the cage. Handling stress dramatically reduced plasma GH levels. Unstressed control females, $n=56$, versus stressed females, $n=48$, $P<0{\cdot}001$; unstressed control males, $n=56$, versus stressed males, $n=49$, $P<0{\cdot}005$; both log-rank test.

as a Cre-lox recombination driver, selectively inhibits GH and IGF-1 signaling (Kappeler *et al.* 2008). These mice have low hypothalamic GHRH during development. Adult bIGF1RKO$^{+/-}$ have small pituitaries (males, 40% smaller than controls; females, 33%; Kappeler *et al.* 2008), fewer somatotroph cells (Fig. 5A), and reduced pituitary GH content (bIGF1RKO$^{+/-}$ males, −80%; females, −81%). To further characterize somatotroph dysfunction in this model, we measured pituitary GH release after *in vivo* stimulation with GHRH. This triggered significant GH secretion in the mutants and control mice, but stimulated GH levels were much lower in bIGF1RKO$^{+/-}$ mice than in controls (bIGF1RKO$^{+/-}$, $26{\cdot}4\pm5{\cdot}6$ versus control, $59{\cdot}7\pm9{\cdot}7$ ng/ml; −44%, $P<0{\cdot}01$; Fig. 5B). We then investigated how the somatotropic deficiency in bIGF1RKO$^{+/-}$ mice affected endogenous GH secretion. Analyzing GH distribution pattern revealed significantly lower GH levels in the mutants ($P<0{\cdot}001$ in both sexes; log-rank test; Fig. 5C): 75% of the GH values in bIGF1RKO$^{+/-}$ females were under 2·0 ng/ml versus 40% in the controls ($\chi^2=25{\cdot}1$, $P<0{\cdot}001$); in males, 85% of the GH values in the mutants were under 2·0 ng/ml versus 56% in the controls ($\chi^2=20{\cdot}2$, $P<0{\cdot}001$). Nevertheless, some very high peak values were also found in the mutants. To check whether the observed differences might be explained by any particular stress in the mutants, we measured ACTH levels, but found no change in basal hormone levels or under stress (Fig. 5D).

GHR/Jak2/Stat5 pathway activation correlates with GH levels in mice

Peripheral GHR and GHR-dependent Jak2/Stat5 signaling pathways are activated within minutes after GH peaks in the circulation (Tannenbaum *et al.* 2001, Verma *et al.* 2005, Dhir *et al.* 2007). We showed previously that in wild-type mice, Jak2 activation in the liver is completed 2 min after GH injection into the portal vein (Kappeler *et al.* 2008). Since this delay is short compared with the time course of GH peaks, the degree of GHR/Jak2/Stat5 activation may actually correlate closely with the plasma GH concentration in mice. To investigate this, we drew blood from unstressed wild-type mice and took liver and skeletal muscle biopsies 2 min later. We then ranked these individuals by their plasma GH levels and defined four subgroups: G1–G4 (see Fig. 6A). Measuring tyrosine phosphorylation of GHR (pGHR), Jak2 (pJak2), and Stat5 (pStat5), we found a significant increase in GHR/Jak2/Stat5 pathway activation

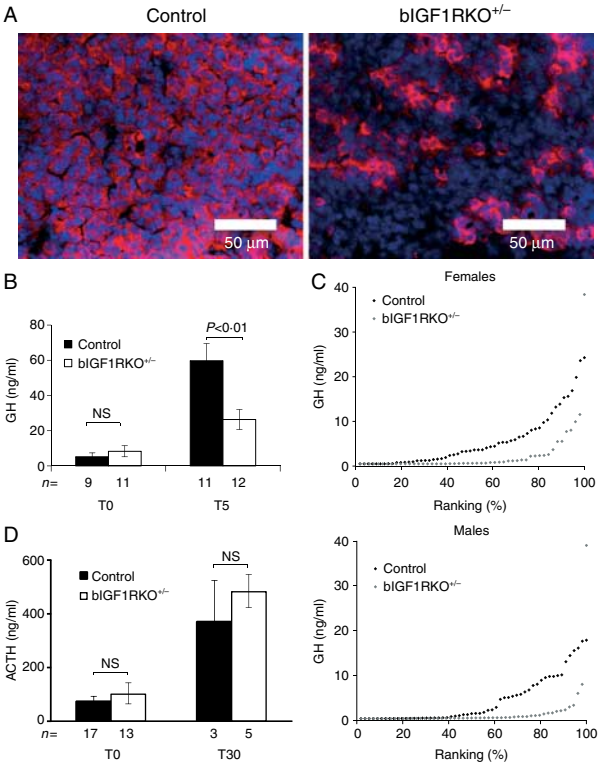

Figure 5 Abnormal GH secretion in bIGF1RKO$^{+/-}$ mutants. (A) Immunodetection of somatotroph cells (red) in pituitary sections from 3-month-old control and bIGF1RKO$^{+/-}$ males showed lack of GH containing cells in mutant mice. Scale bar, 50 µm. Blue, DAPI nuclear stain. (B) GH release test in 6-month-old bIGF1RKO$^{+/-}$ and control males. Recombinant mGHRH was i.p. injected into anesthetized adult males. Plasma GH was measured at the time of injection (T0 group) and after 5 min (T5 group). GH at T0 was slightly elevated with respect to the profiles in Fig. 3, due to pentobarbital anesthesia (Saito *et al.* 1979). bIGF1RKO$^{+/-}$ mutants showed insufficient GH secretion after GHRH administration ($P<0{\cdot}01$, the Mann–Whitney *U* test). (C) GH levels were significantly lower in bIGF1RKO$^{+/-}$ mice, with fewer intermediate and peak GH values. Control values shown here are the same as those in Fig. 3A. All animals were unstressed. Control females, $n=56$; bIGF1RKO$^{+/-}$ females, $n=52$; $P<0{\cdot}001$; control males, $n=56$; bIGF1RKO$^{+/-}$ males, $n=54$; $P<0{\cdot}01$; both log-rank test. (D) We measured ACTH in unstressed (T0) and stressed (T30) control and mutant mice (6-month-old), and found it strongly elevated in the stressed group, as expected. No significant difference existed between genotypes. NS, not significant.

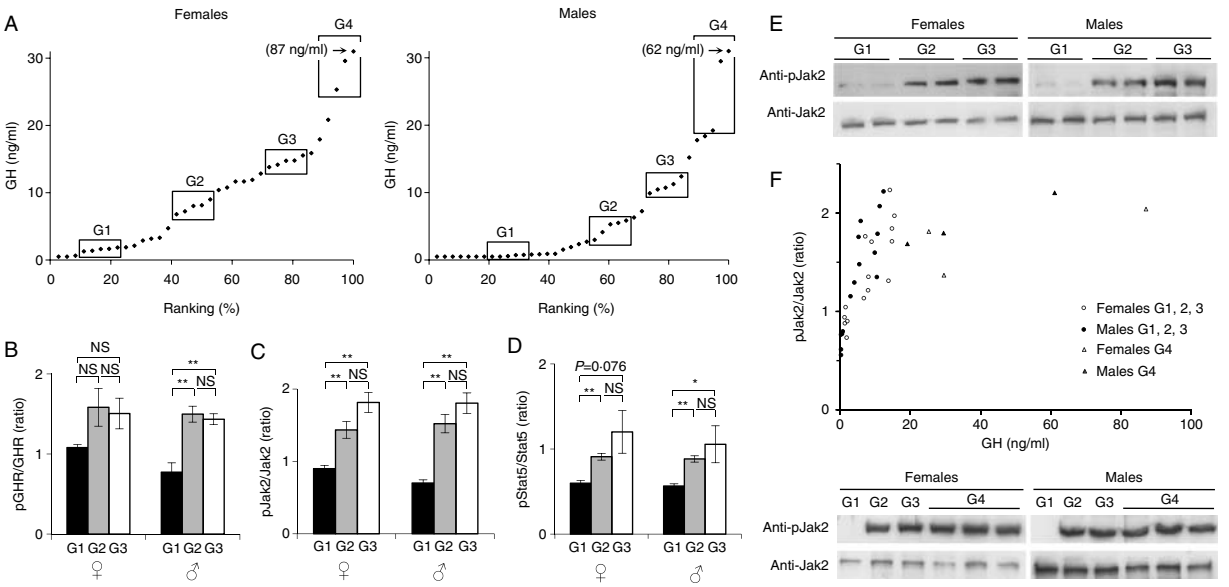

Figure 6 Activation of the GHR/Jak2/Stat5 pathway in response to endogenous GH. (A) GH measurements were performed in blood samples from male and female wild-type mice. A strong tendency to low nadir levels in males was confirmed ($P=0{\cdot}02$, the Wilcoxon signed-rank test). For males and females, we then defined four subgroups according to GH levels: group 1 (G1) with nadir GH, G2 with low GH, G3 with high GH, and G4 representing peaks. (B–D) We then determined activated GHR (pGHR), pJak2, and pStat5 levels from liver samples of G1–G3 animals by western blot. Significant differences in pathway activation existed between nadir and low GH levels (G1 versus G2); $n=5$ per group; $^{*}P<0{\cdot}05$; $^{**}P<0{\cdot}01$; NS, not significant; the Mann–Whitney *U* test. (E) Representative western blots of pJak2 detection (panel C). Equivalent results were obtained for pGHR and pStat5. (F) Upper panel: scatter plot of liver pJak2 from panel (C), together with the G4 individuals (triangles). Jak2 activation during GH peak (G4) was not higher than under high GH (G3). Lower panel: representative western blots.

from nadir to low GH levels (comparing G1 with G2; Fig. 6B–E). From low to high GH levels (G2–G3), the pJak2 and pStat5 activation levels tended to increase further, but differences were not statistically significant (Fig. 6B–E). Since subgroups G1–G4 cannot be compared directly across the sexes (because of different average GH levels), we analyzed the results in a scatter plot. This revealed a strong correlation between pJak2 and plasma GH between 0·5 and 20 ng/ml for females (slope $=0{\cdot}07$, $R=0{\cdot}73$, $n=15$, $P<0{\cdot}001$) and for males (slope $=0{\cdot}11$, $R=0{\cdot}77$, $n=15$, $P<0{\cdot}001$; Fig. 6F). Surprisingly, GH at peak values (G4; 19·2–87·1 ng/ml) did not show higher Jak2/Stat5 pathway activation than already obtained under high GH levels (G3). We repeated this analysis in muscle, with similar result (not shown).

Discussion

Serial sampling by catheterization is the method of choice and gold standard for studying pulsatile GH secretion. This method, however, is difficult to implement in mouse, and only one group have reported on pulsatile GH profiles in mice (MacLeod *et al.* 1991, Pampori & Shapiro 1994). In this study, we have developed a method that avoids the cumbersome cannulation in small animals. We sampled blood randomly in cohorts of mice, and arranged the data as rank plots. Comparing such data from groups of mice using log-rank and the Wilcoxon signed-rank test provided key information on GH release and somatotropic function. A powerful Approximate Entropy approach has been developed by Pincus (1991) and is used to evaluate irregularity of GH secretion (Pincus *et al.* 1996). However, characteristics other than irregularity are also important. In this study, we have focused on analyzing the distribution of GH concentrations, which is readily affected by mutations and treatments. Data from Low *et al.* (2001) and Yakar *et al.* (2001) on SST and LID mutant mice respectively had shown several-fold increase in average GH levels and absence of nadir values in mutants. In such cases of extreme oversecretion, GH data from spot samples can be directly compared. However, when changes are less dramatic, rank plot analysis is particularly helpful, and we propose to systematically use this approach together with log-rank or the Wilcoxon signed-rank test to evaluate GH secretion from spot samples.

To detect pulses in serial analysis in rodents, sample intervals must be 20 min or less and collected over at least 8 h to include a minimum of two peaks. Thus, the lower limit for serial GH analysis is 24 samples, per individual. In serial and random sampling, about 10% of the GH values from wild-type animals correspond to the steep parts of the peak, while the intermediate GH levels – which represent about half of the values – correspond to small peaks or

the ascending/descending phases of high peaks (compare Figs 1 and 3). Based on this prevalence, statistical sample size estimation showed that about 30 determinations suffice to include elevated peak values with high probability. In practice, a representative nadir-to-peak distribution can be achieved with 30 samples, and rank plots are optimal with 50 samples. For statistical analysis, if differences in GH are several-fold and concern all parts of the ranked distribution, a nonparametric Mann–Whitney *U* test is sufficient. If the distribution of ranked data are to be compared, log-rank test is appropriate. If differences are mainly occurring among nadir levels, the Wilcoxon rank test should be applied to focus on comparing the nadir part of the distribution. Finally, the high 10% of the GH values can be evaluated separately by establishing linear regression. Parameters from linear regression can then be compared between mutant (or treatment) and controls, providing useful indication on prevalence, height, and broadness of peaks (not shown).

We explored the GH patterns in wild-type mice and found them similar to rats (Pincus *et al.* 1996, Giustina & Veldhuis 1998, Veldhuis *et al.* 2008). Importantly, the low nadir level – a key feature of male GH secretion – was readily picked up by rank plot analysis. This was the case when we revised the data from Pincus *et al.* (1996), and also when we explored ours. However, it is true that values from small and large peaks overlap in rank plot and that no clear-cut boundaries exist. Thus, rank plots allowed revealing sex differences with respect to nadir levels, but they were less sensitive concerning other known gender-related differences. Consistent with the findings from rats, we saw no significant nycthemeral differences in the GH profile in male mice. Females, in contrast, showed strong nycthemeral differences. However, GH was higher during the light period, which contrasts with the published data in rats. Interestingly, MacLeod *et al.* (1991) demonstrated that females have more peaks than males during the day, which is consistent with the elevated daylight GH levels of females in this study. Finally, the fact that differences between males and females in our rank plots are not as obvious as, for instance, in Fig. 1 could be due to the lower number of data points or the less sensitive GH assay. Indeed, nadir differences are equally interesting as peak values and using an assay with higher sensitivity should be considered. Moreover, it needs to be stressed that we analyzed GH in samples taken from multiple mice, thereby introducing inter-individual variation, while data in Fig. 1 compare only one male and female (see also Supplementary Figure 2, see section on supplementary data given at the end of this article).

Rank plots reveal the effect of stress on GH release in mice

Routine animal care, such as handling and change, causes stress and leads to marked changes in plasma hormone levels (Balcombe *et al.* 2004). Brown & Martin (1974) showed that in rat, plasma corticosterone increases and GH levels drop quickly after exposure to handling stress. Using rank plot analysis, we showed that mice are sensitive to handling and that cage opening was sufficient to initiate a dramatic drop in plasma GH within minutes. Even in the bIGF1RKO$^{+/-}$ mice, which present with GH release deficiency (Fig. 5), cage opening and handling further suppressed the plasma GH levels (not shown). This rapid GH decrease can be explained by the short initial half-life of plasma GH, which is 2·2 min in mice (Turyn & Bartke 1993) and 3·3 min in rats (Chapman *et al.* 1991). We conclude that wherever the mice are – in a peak or in an intermediate part of the curve – stress immediately stops secretion and GH levels fall very quickly due to the extremely short half-life of the hormone. Uptake of GH by the liver, in contrast, does not seem to play a role (Turyn *et al.* 1997). Interestingly, some peaks seemed resistant to stress. Consequently, to measure undisturbed GH levels, blood samples must be taken immediately upon cage opening. To further explore this swift response to stress, we reduced the time between moving the mouse and drawing blood to <20 s (experiment shown in Fig. 6A), which is roughly the time the blood needs for one circulation. Under these conditions, the overall GH distribution pattern remained the same, but the GH levels (see Fig. 6A) were on average higher than in Fig. 3, where blood was sampled within the first 2 min after cage opening. A rough estimation indicates that 40 s after starting animal handling, about 10% of the original endogenous GH is lost, and that after 1 min, this reduction may reach 20%. After 3 min, about two thirds of the original GH concentration was lost. Serial GH determination in mice by MacLeod *et al.* (1991) revealed a relative absence of intermediate levels, which becomes evident when data are transformed into rank plot (Supplementary Figure 2, see section on supplementary data given at the end of this article). While this particularity may be due to genetic background, it could also represent an effect of stress, similar to that reported in this study in Fig. 4. It is indeed possible that the pulses reported by MacLeod *et al.* correspond to the peaks that we found resistant to stress. However, these authors also showed that catheterization alone did not lead to higher stress hormone levels (MacLeod & Shapiro 1988). On the other hand, the repeated loss of blood volume itself could trigger a stress response. While it is difficult to conclude from the few existing data, these findings underscore the interest in further exploring GH pulsatility in mice. In particular, the high proportion of intermediate GH concentrations detected in spot samples from wild-type mice using rank plot analysis merits further investigation.

Rank plot analysis of endocrine GH deficiency caused by brain IGF-1R knockout

We reported that inactivation of IGF-1R in the embryonic brain (bIGF1RKO$^{+/-}$) selectively inhibits GH and IGF-1 signaling, and that low GHRH levels are involved (Kappeler *et al.* 2008). The bIGF1RKO$^{+/-}$ mutants show depletion of pituitary GH, low circulating IGF-1, and delayed somatic growth: at 3 months of age they weigh 10% less than controls.

The bIGF1RKO$^{+/-}$ pituitaries are smaller, display low somatotroph density, and were less responsive to GHRH stimulation. Together, these results indicated that the initial developmental defect of the hypothalamo-pituitary axis led to adult GH secretory dysfunction. Using rank plot analysis in bIGF1RKO$^{+/-}$ mice we showed that the hypothalamo-pituitary changes resulted in strongly reduced plasma GH. The GH pattern showed rarefied peak and more frequent trough values, suggesting that broadness and/or number of peaks were reduced in the mutants, in accordance with their diminished GHRH levels. This relationship between rank plot distribution and underlying pulsatility has been explored in Fig. 2. In bIGF1RKO$^{+/-}$ mouse model, the marked GH deficiency in juvenile mutants is associated with reduced age-related mortality and increased lifespan. This phenotype is consistent with the findings from other long-lived mouse strains (Kenyon 2001, 2005, and references therein). Since little is known about GH release pattern in these models, we suggest exploring circulating GH in these models to gain more insight into the physiopathology of somatotropic signaling involved in mammalian longevity.

Plasma GH and Jak/Stat pathway activation

We investigated the activation of the GHR/Jak2/Stat5 pathway in the liver exposed to different levels of circulating GH, and found a strong correlation between circulating GH and the degree of GHR, Jak2, and Stat5 phosphorylation. This was true for GH concentrations between nadir and high GH. Similar correlation between the GH concentration and degree of Stat5 activation has been shown in rats (Choi & Waxman 2000*a*). The G2, G3, and G4 values (see Fig. 6) are all part of a GH pulse and it is not possible to know whether these elevated values are close to a peak or still in the ascending/descending phase of a peak. However, we demonstrated previously that Jak2 activation in wild-type mice is complete just 2 min after i.v. bolus of GH. Recently, Verma *et al.* (2005) showed in hypophysectomized rats that i.v. GH injection activated the Jak/Stat pathway within minutes. Importantly, we did not observe combinations of high pathway activation and low GH levels or vice versa.

Concerning GH-deficient bIGF1RKO$^{+/-}$ mutants, we showed previously that GHR and Jak2 in the liver are hypersensitive to exogenous GH (Kappeler *et al.* 2008). In this study, we found that liver GHR, Jak2, and Stat5 were phosphorylated to some degree at nadir GH concentrations. Together, this could partly compensate for the reduced GH levels and explain why the growth deficit in bIGF1RKO$^{+/-}$ mutants is relatively small compared to complete GHR knockout: adult body weight in mice with constitutive GHRKO is about 40% lower than in controls, whereas adult body weight in bIGF1RKO$^{+/-}$ mice is only 10% less than controls (Kappeler *et al.* 2008, Berryman *et al.* 2010). Thus, it seems that even low GH concentrations together with rare peaks can support significant somatic growth.

Interestingly, the highest GH peaks that we observed (G4 in Fig. 6) did not further increase the Jak/Stat pathway activation, similar to the published data (Choi & Waxman 2000*a*). We suggest that the intermediate GH levels are of prime importance in the regulation of GHR pathway activation. Finally, the elevated nadir levels in females did not translate into higher Jak/Stat pathway activation, similar to rat (Choi & Waxman 1999). Similarly, male G2 and female G2 showed the same degree of activation, although GH levels in the female G2 were higher than in males (compare Fig. 6C–F). This suggests that females are somewhat resistant to endogenous GH compared to males. Others showed that Stat5b activates gender-specific gene expression in the liver in response to sex-dimorphic GH pattern (Choi & Waxman 2000*b*, Waxman & O'Connor 2006), a fact that is compatible with our data. Studying these mechanisms using rank plot analysis may provide new insight into how sex-dimorphic gene expression is controlled by pulsatile somatotropic signaling in mice.

In conclusion, we propose a method that facilitates the study of GH release patterns in mice. This method provides insight into key aspects of GH release and is helpful in those small animals where obtaining serial data via cannulation is problematic. Indeed, rank plot analysis makes a valid statement about circadian endogenous GH levels, while serial data from mice reveal peak frequency. Using rank plots, we explored the acute effects of stress on circulating GH and the effects of GH on downstream signaling pathways. We also showed that extended periods of trough GH are associated with extended lifespan in mice, providing further evidence for the critical role of GH signaling in aging and longevity determination. It is noteworthy to say that other pulsatile hormones can also be studied using rank plot analysis.

Supplementary data

This is linked to the online version of the paper at http://dx.doi.org/10.1677/JOE-10-0317.

Declaration of interest

The authors declare that there is no conflict of interest that could be perceived as prejudicing the impartiality of the research reported.

Funding

The ANR (grant NT05-3 42491), the EU Network of Excellence LifeSpan (036894), and the GIS Institut du Vieillissement sponsored this study with grants to MH; the ARC, Inserm, and MENRT supported LK and CDMF.

Author contribution statement

MH designed, AJB, CDMF, JD, MH, and LK performed the experiments. JX analyzed the data and wrote the manuscript. SR and IAM performed statistical evaluation. All authors discussed the results and commented on the manuscript.

Acknowledgements

We thank I Renault and N R Holzenberger for their dedicated help with *in vivo* experiments, Alex Edelman and Associates (SARL) for language revision, G Thordarson, G Gudmundur, and F Talamantes for antibodies, and J Solinc for assistance with statistical analysis.

References

Balcombe JP, Barnard ND & Sandusky C 2004 Laboratory routines cause animal stress. *Contemporary Topics in Laboratory Animal Science* **43** 42–51.

Bartke A 2003 Is growth hormone deficiency a beneficial adaptation to aging? Evidence from experimental animals *Trends in Endocrinology and Metabolism* **14** 340–344. (doi:10.1016/S1043-2760(03)00115-2)

Bartke A 2008 Impact of reduced insulin-like growth factor-1/insulin signaling on aging in mammals: novel findings. *Aging Cell* **7** 285–290. (doi:10.1111/j.1474-9726.2008.00387.x)

Berryman DE, List EO, Palmer AJ, Chung MY, Wright-Piekarski J, Lubbers E, O'Connor P, Okada S & Kopchick JJ 2010 Two-year body composition analyses of long-lived GHR null mice. *Journals of Gerontology Series A: Biological Sciences and Medical Sciences* **65** 31–40. (doi:10.1093/gerona/glp175)

Brown GM & Martin JB 1974 Corticosterone, prolactin, and growth hormone responses to handling and new environment in the rat. *Psychosomatic Medicine* **36** 241–247.

Brown-Borg HM, Borg KE, Meliska CJ & Bartke A 1996 Dwarf mice and the ageing process. *Nature* **384** 33. (doi:10.1038/384033a0)

Chapman IM, Helfgott A & Willoughby JO 1991 Disappearance half-life times of exogenous and growth hormone-releasing factor-stimulated endogenous growth hormone in normal rats. *Journal of Endocrinology* **128** 369–374. (doi:10.1677/joe.0.1280369)

Choi HK & Waxman DJ 1999 Growth hormone, but not prolactin, maintains, low-level activation of STAT5a and STAT5b in female rat liver. *Endocrinology* **140** 5126–5135. (doi:10.1210/en.140.11.5126)

Choi HK & Waxman DJ 2000*a* Plasma growth hormone pulse activation of hepatic JAK–STAT5 signaling: developmental regulation and role in male-specific liver gene expression. *Endocrinology* **141** 3245–3255. (doi:10.1210/en.141.9.3245)

Choi HK & Waxman DJ 2000*b* Pulsatility of growth hormone (GH) signalling in liver cells: role of the JAK–STAT5b pathway in GH action. *Growth Hormone and IGF Research* **10** (Supplement B) S1–S8. (doi:10.1016/S1096-6374(00)80002-7)

Coschigano KT, Clemmons D, Bellushi LL & Kopchick JJ 2000 Assessment of growth parameters and life span of GHR/BP gene-disrupted mice. *Endocrinology* **141** 2608–2613. (doi:10.1210/en.141.7.2608)

Coschigano KT, Holland AN, Riders ME, List EO, Flyvbjerg A & Kopchick JJ 2003 Deletion, but not antagonism, of the mouse growth hormone receptor results in severely decreased body weights, insulin, and insulin-like growth factor I levels and increased life span. *Endocrinology* **144** 3799–3810. (doi:10.1210/en.2003-0374)

Dhir RN, Thangavel C & Shapiro BH 2007 Attenuated expression of episodic growth hormone-induced CYP2C11 in female rats associated with suboptimal activation of the Jak2/Stat5B and other modulating signaling pathways. *Drug Metabolism and Disposition* **35** 2102–2110. (doi:10.1124/dmd.107.017475)

Dupont J, Karas M & LeRoith D 2000 The potentiation of estrogen on insulin-like growth factor I action in MCF-7 human breast cancer cells includes cell cycle components. *Journal of Biological Chemistry* **275** 35893–35901. (doi:10.1074/jbc.M006741200)

Flurkey K, Papaconstantinou J, Miller RA & Harrison DE 2001 Lifespan extension and delayed immune and collagen aging in mutant mice with defects in growth hormone production. *PNAS* **98** 6736–6741. (doi:10.1073/pnas.111158898)

Giustina A & Veldhuis JD 1998 Pathophysiology of the neuroregulation of growth hormone secretion in experimental animals and the human. *Endocrine Reviews* **19** 717–797. (doi:10.1210/er.19.6.717)

Godfrey P, Rahal JO, Beamer WG, Copeland NG, Jenkins NA & Mayo KE 1993 GRH receptor of little mice contains a missense mutation in the extracellular domain that disrupts receptor function. *Nature Genetics* **4** 227–232. (doi:10.1038/ng0793-227)

Holzenberger M, Dupont J, Ducos B, Leneuve P, Geloen A, Even PC, Cervera P & Le Bouc Y 2003 IGF-1 receptor regulates life span and resistance to oxidative stress in mice. *Nature* **421** 182–187. (doi:10.1038/nature01298)

Kappeler L, Zizzari P, Alliot J, Epelbaum J & Bluet-Pajot MT 2004 Delayed age-associated decrease in growth hormone pulsatile secretion and increased orexigenic peptide expression in the Lou C/JaLL rat. *Neuroendocrinology* **80** 273–283. (doi:10.1159/000083610)

Kappeler L, De Magalhaes Filho C, Dupont J, Leneuve P, Cervera P, Périn L, Loudes C, Blaise A, Klein R, Epelbaum J *et al.* 2008 Brain IGF-1 receptors control mammalian growth and lifespan through a neuroendocrine mechanism. *PLoS Biology* **6** 2144–2153. (doi:10.1371/journal.pbio.0060254)

Kappeler L, De Magalhaes Filho C, Leneuve P, Xu J, Brunel N, Chatziantoniou C, Le Bouc Y & Holzenberger M 2009 Early postnatal nutrition determines somatotropic function in mice. *Endocrinology* **150** 314–323. (doi:10.1210/en.2008-0981)

Kenyon C 2001 A conserved regulatory system for aging. *Cell* **105** 165–168. (doi:10.1016/S0092-8674(01)00306-3)

Kenyon C 2005 The plasticity of aging: insights from long-lived mutants. *Cell* **120** 449–460. (doi:10.1016/j.cell.2005.02.002)

Low MJ, Otero-Corchon V, Parlow AF, Ramirez JL, Kumar U, Patel YC & Rubinstein M 2001 Somatostatin is required for masculinization of growth hormone-regulated hepatic gene expression but not of somatic growth. *Journal of Clinical Investigation* **107** 1571–1580. (doi:10.1172/JCI11941)

MacLeod JN & Shapiro BH 1988 Repetitive blood sampling in unrestrained and unstressed mice using a chronic indwelling atrial catheterization apparatus. *Laboratory Animal Science* **38** 603–608.

MacLeod JN, Pampori NA & Shapiro BH 1991 Sex differences in the ultradian pattern of plasma growth hormone concentrations in mice. *Journal of Endocrinology* **131** 395–399. (doi:10.1677/joe.0.1310395)

Pampori NA & Shapiro BH 1994 Effects of neonatally administered monosodium glutamate on the sexually dimorphic profiles of circulating growth hormone regulating murine hepatic monooxygenases. *Biochemical Pharmacology* **47** 1221–1229. (doi:10.1016/0006-2952(94)90394-8)

Pincus SM 1991 Approximate entropy as a measure of system complexity. *PNAS* **88** 2297–2301. (doi:10.1073/pnas.88.6.2297)

Pincus SM, Gevers EF, Robinson IC, van den Berg G, Roelfsema F, Hartman ML & Veldhuis JD 1996 Females secrete growth hormone with more process irregularity than males in both humans and rats. *American Journal of Physiology* **270** E107–E115.

Saito H, Ogawa T, Ishimaru K, Oshima I & Saito S 1979 Effect of pentobarbital and urethane on the release of hypothalamic somatostatin and pituitary growth hormone. *Hormone and Metabolic Research* **11** 550–554. (doi:10.1055/s-0028-1092778)

Selman C, Lingard S, Choudhury AI, Batterham RL, Claret M, Clements M, Ramadani F, Okkenhaug K, Schuster E, Blanc E *et al.* 2008 Evidence for lifespan extension and delayed age-related biomarkers in insulin receptor substrate 1 null mice. *FASEB Journal* **22** 807–818. (doi:10.1096/fj.07-9261com)

Taguchi A, Wartschow LM & White MF 2007 Brain IRS2 signaling coordinates life span and nutrient homeostasis. *Science* **317** 369–372. (doi:10.1126/science.1142179)

Tannenbaum GS, Choi HK, Gurd W & Waxman DJ 2001 Temporal relationship between the sexually dimorphic spontaneous GH secretory profiles and hepatic STAT5 activity. *Endocrinology* **142** 4599–4606. (doi:10.1210/en.142.11.4599)

Tronche F, Kellendonk C, Kretz O, Gass P, Anlag K, Orban PC, Bock R, Klein R & Schütz G 1999 Disruption of the glucocorticoid receptor gene in the nervous system results in reduced anxiety. *Nature Genetics* **23** 99–103. (doi:10.1038/12703)

Turyn D & Bartke A 1993 Pharmacokinetics of radioiodinated human and ovine growth hormones in transgenic mice expressing bovine growth hormone. *Transgenic Research* **2** 219–226. (doi:10.1007/BF01977352)

Turyn D, Dominici FP, Sotelo AI & Bartke A 1997 Growth hormone-binding protein enhances growth hormone activity *in vivo*. *American Journal of Physiology* **273** E549–E556.

Veldhuis JD, Keenan DM & Pincus SM 2008 Motivations and methods for analyzing pulsatile hormone secretion. *Endocrine Reviews* **29** 823–864. (doi:10.1210/er.2008-0005)

Verma AS, Dhir RN & Shapiro BH 2005 Inadequacy of the Janus kinase 2/signal transducer and activator of transcription signal transduction pathway to mediate episodic growth hormone-dependent regulation of hepatic CYP2C11. *Molecular Pharmacology* **67** 891–901. (doi:10.1124/mol.104.005454)

Waxman DJ & O'Connor C 2006 Growth hormone regulation of sex-dependent liver gene expression. *Molecular Pharmacology* **20** 2613–2629. (doi:10.1210/me.2006-0007)

Yakar S, Liu JL, Fernandez AM, Wu Y, Schally AV, Frystyk J, Chernausek SD, Mejia W & Le Roith D 2001 Liver-specific igf-1 gene deletion leads to muscle insulin insensitivity. *Diabetes* **50** 1110–1118. (doi:10.2337/diabetes.50.5.1110)

Received in final form 12 October 2010
Accepted 2 November 2010
Made available online as an Accepted Preprint
2 November 2010